A Bow Echo and Severe Weather Associated with a Kona Low in Hawaii

STEVEN BUSINGER AND THOMAS BIRCHARD JR.

University of Hawaii, Honolulu, Hawaii

KEVIN KODAMA*

Joint Institute for Marine and Atmospheric Research, Honolulu, Hawaii

PAUL A. JENDROWSKI

National Weather Service Forecast Office, Honolulu, Hawaii

JIAN-JIAN WANG+

UCAR COMET Outreach Program, Boulder, Colorado

(Manuscript received 23 April 1997, in final form 21 November 1997)

ABSTRACT

On 2 November 1995 a kona low formed to the northwest of Hawaii. During the following 48 h a series of convective rainbands developed on the southeastern side of the low as it slowly moved eastward. On the afternoon of 3 November 1995 Hawaiian standard time (HST), a bow-echo signature was identified in the reflectivity observations from the recently installed WSR-88D located on the south shore of Kauai, and led to the first severe thunderstorm warning ever issued by the National Weather Service Forecast Office in Honolulu, Hawaii. Subsequent to the warning, winds of 40 m s^{-1} (80 kt) were observed at Nawiliwili Harbor on the southeast side of Kauai. The goals of this paper were to (i) document, within the constraints of the observational data, the synoptic and mesoscale environment associated with the formation of the bow echo and severe weather in Hawaii and contrast them with investigations of similar phenomena in the midlatitudes and Tropics, and (ii) provide a discussion of the implications of the availability of data from the new WSR-88D radars in Hawaii to operational forecasting of severe weather in the central Pacific.

1. Introduction

Despite its reputation for benign tranquillity, punctuated only by brief tropical showers, the atmosphere over Hawaii can produce surprisingly violent storms. This is a fact that did not escape the islands' earliest inhabitants and is much on the minds of operational forecasters working in the Pacific region (Kodama and Businger 1998, this issue):

> Coming is the dark cloud and the rainbow;
> Wildly comes the rain and the wind;
> Whirlwinds sweep over the earth;
> Rolling down are the rocks of the ravines;
> The red mountain-streams are rushing to the sea.
> Here are the waterspouts;
> Tumbled about are the clustering clouds of heaven;
> Gushing forth are the springs of the mountains.
>
> [ancient Hawaiian chant describing kona low; Fornander (1996)]

Most notable of these violent storms are hurricanes such as Iniki in 1992. However, from October to April, extratropical weather systems can propagate sufficiently equatorward to substantially alter the dominant, stable trade wind pattern in the vicinity of the Hawaiian Islands.[1] Among these synoptic-scale disturbances is a class of subtropical cyclones known as kona[2] low pressure systems that can produce a wide range of weather

*Current affiliation: National Weather Service Forecast Office, Honolulu, HI.

+Current affiliation: Department of Atmospheric Sciences, University of Illinois at Champaign–Urbana, Urbana, Illinois.

Corresponding author address: Dr. Steven Businger, Department of Meteorology, University of Hawaii, 2525 Correa Rd., Honolulu, HI 96822.
E-mail: businger@soest.hawaii.edu

[1] The Hawaiian Islands range in latitude from ~19° to 22°N, and mean temperatures in summer and winter differ by only a few degrees.

[2] Kona is Hawaiian for leeward, with respect to the usual NE trade wind flow.

hazards, including heavy rains, hailstorms, flash floods, landslides, high winds, large surf and swell, waterspouts, and in the case that is the subject of this paper, severe thunderstorms (Simpson 1952; Ramage 1962; Schroeder 1977a,b; Kodama and Barnes 1997; Ramage 1995).

Most kona lows form from extratropical cyclones that become secluded at lower latitudes by the blocking action of a warm high. Less frequently, kona lows develop from cutoff mid- and upper-tropospheric cold-core lows that extend their circulations to the surface. In both these instances the cold low aloft draws on sources of cold vorticity-rich air from higher latitudes. Kona lows tend to track in slow and erratic loops, resulting in a period of weather characterized by moist south/southwesterly flow and rain squalls, with episodes of high winds and flooding over the Hawaiian Islands that can last for a week or more. A significant fraction of the annual total rainfall on the kona or southwest-facing slopes of the islands can be attributed to the occurrence of a small number of these subtropical lows.

On 2–4 November 1995, a kona low evolved from an occluded wave cyclone and spawned a series of squall lines as it approached the Hawaiian Islands from the northwest. As one of these convective bands approached the island of Kauai, it exhibited a pronounced bow-echo structure (Nolen 1959; Fujita 1978) in reflectivity observations with the recently installed Weather Surveillance Radar-1988 Doppler (WSR-88D) radar located on the south side of the island of Kauai. Recognition of the implications of the radar data led to the issuance of a severe thunderstorm warning, the first such warning ever issued by the National Weather Service Forecast Office in Honolulu, Hawaii (WFSO HNL) (see appendix A). Subsequent to the warning, winds of 40 m s^{-1} (80 kt) were observed at Nawiliwili Harbor on the southeast side of Kauai and convective-scale wind gusts tore the roof off the Nawiliwili Small Boat Harbor office and knocked down trees and power lines across portions of south and east Kauai. Radar in this case provided critical lead time for the issuance of a severe thunderstorm warning that was subsequently verified and provides the data for the mesoscale postanalysis presented here.

The idealized evolution of an isolated, or single-cell type, bow echo is described by Fujita (1978). During the most intense phase, the center of the bow forms a spearhead, with cyclonic and anticyclonic rotation at the ends of the bow. Rear inflow notches along the trailing edge of the line segment usually indicate where the strongest downburst winds are located. Rear inflow notches are a result of rear inflow jets that appear to form bow echoes by differentially advecting a part of the squall line or thunderstorm cell forward, and by entraining dry, lower θ_e air into the rear flank, which then erodes the back side of the advancing bow echo through the evaporation of hydrometeors.

Observational studies and numerical simulations have been utilized to determine the dynamics of rear inflows that characterize bow-echo mesoconvection in midlatitudes (Lee et al. 1992; Weisman 1992, 1993; Johns 1993; Skamarock et al. 1994; Przybylinski 1995; Knupp 1996; among others). Johns and Hirt (1987) observed that bow echoes associated with widespread damaging winds (derechos) east of the Rocky Mountains can occur with either strong, migrating low pressure systems (called the ''dynamic'' pattern) or with weather patterns exhibiting relatively weak synoptic-scale features (called the ''warm season'' pattern). Moreover, Johns (1993) noted that individual bow echoes and bowing line segments can form in a wide variety of synoptic environments.

There have also been a considerable number of observational and numerical modeling studies of tropical squall lines (Aspliden et al. 1976; Houze 1977; Zipser 1977; Barnes and Sieckman 1984; Chong et al. 1987; Nicholls 1987; Roux and Ju 1990; Keenan and Carbone 1992; Trier et al. 1996, 1997; Jorgensen et al. 1997). The majority of tropical squall lines studied propagate from east to west, and those exhibiting greater low-level wind shear tend to propagate faster than those with weaker wind shear (Barnes and Sieckman 1984). The majority of midlatitude squall lines propagate from west to east consistent with the prevailing low-level winds in the midlatitude and tropical latitude belts.

The growth, intensity, and dynamics of tropical and midlatitude squall lines have been related to environmental thermodynamic instability and vertical shear of the horizontal winds in the lower troposphere (e.g., Weisman and Klemp 1982; Barnes and Sieckman 1984). The observation of a variety of organized mesoscale convective systems has led to a classification method that relates storm severity to the bulk Richardson number ($R_i = B/0.5U^2$, where B is the buoyant energy in the storm's environment and U is a measure of the vertical wind shear). The combination of higher convective available potential energy (CAPE) and shear values is associated with midlatitude supercells and tornadic storms, whereas tropical squall lines typically exhibit lower CAPE and shear values (Keenan and Carbone 1992).

A squall line over the western tropical Pacific Ocean documented by Jorgensen et al. (1997) moved west to east and exhibited a bow-shaped radar reflectivity structure. A mesoscale vortex developed as the reflectivity signature became increasingly bow shaped. The associated CAPE value in their case was $\sim$1500 J kg^{-1} and the environmental hodograph showed a 12 m s^{-1} westerly jet at $\sim$2 km, with little directional shear up to $\sim$5 km. A recent paper by Alfonso and Naranjo (1996) describes a serial bow echo, or derecho, that formed in a baroclinic environment of a midlatitude low pressure system that affected Cuba, demonstrating the penetration of an essentially midlatitude phenomena to subtropical latitudes. This paper provides the first documentation of a bow echo in association with a subtrop-

ical or kona low, in an ocean environment far removed from continental landmasses.

The goals of this paper are to discuss the implications of the availability of data from the new WSR-88D radars in Hawaii to operational forecasting of severe weather in the central Pacific and to document, within the constraints of the observational data, the synoptic and mesoscale environment associated with the formation of the Hawaiian bow echo.

2. Synoptic setting

It is always challenging to accurately analyze the location and intensity of storm systems over the central Pacific Ocean because of the lack of in situ data. Upper-air analyses (Fig. 1) are based on the initialization of the Aviation (AVN) run of the Global Spectral Model (GSM) and have the benefit of the prior information content of the model and aircraft and satellite data input over the ocean. Surface analyses (Fig. 2) include all operationally available and archived ship-based observations obtained from the National Climatic Data Center. Critical sounding data from Lihue, Kauai, on the day of the bow echo are missing due to a lightning strike at the radiosonde release site. The last available sounding was for 0000 UTC on 3 November 1995, whereas the bow echo formed at ~0200 UTC on 4 November 1995. Therefore, in the vicinity of the bow echo, output from the National Centers for Environmental Prediction's Regional Spectral Model (RSM) (Juang and Kanamitsu 1994) are utilized to infer some meso-alpha-scale features associated with the bow-echo environment. The RSM output utilized in this paper is based on the first nest of the model, with 25-km resolution. Wang et al. (1998, in this issue) describe in detail the operational[3] and case study use of the RSM in Hawaii and provide additional documentation of the RSM simulation of this bow echo case. The RSM simulation did produce a banded maximum in the rainfall just west of Kauai (Wang et al. 1998, Fig. 6b), generally consistent with radar data. However, the RSM did not capture mesoscale details of the bow-echo development; thus, only those model structures that are generally consistent with other data sources (satellite and radar) are cautiously presented in this section.

The kona low developed from a wave cyclone on 2 November 1995. As the wave cyclone occluded, high pressure to the west moved northeastward, secluding the storm from the westerlies and the source of cold air to the north. At 0000 UTC 3 November 1995, a high-amplitude, cold-core low is seen in the 250-hPa analysis along 170°W longitude (Fig. 1a). A region of enhanced divergence aloft can be seen northwest of the islands. A short-wave–jet streak with winds of 70 m s^{-1} on the west side of the trough axis aloft (Fig. 1a) causes the trough to propagate equatorward and increases upper-level divergence over the Hawaiian Islands during the ensuing 24 h (Fig. 1b). A region of subsiding, dry air is seen in the *GOES-9* water vapor imagery for 0101 UTC 3 November on the west side of the cold low aloft (Fig. 3a). In the southeast quadrant of the kona low, alternating bands of dry and moist air with convective anvils are seen in the water vapor image (Fig. 3a), and cold cloud tops (≤ -70°C) associated with the anvils from bands of convective thunderstorms are present in infrared imagery at the same time (not shown). The sea level pressure analysis for 0000 UTC 3 November shows a 989-hPa cyclone center near 36°N and 164°W (Fig. 2a). On the southeast side of the low, confluent inflow feeds moist air into the low, whereas on the southwest side of the low the airflow is diffluent. The trailing anticyclone, with a central pressure of 1032 hPa, is located near 47°N and 177°E and is tracking northeastward.

The atmospheric sounding from Lihue, Kauai, at 0000 UTC 3 November 1995 (Fig. 4) is moist and unstable, with a lifted index of -5 and CAPE of 2364 J kg^{-1}. The vertical wind profile shows veering and considerable low-level vertical shear of the horizontal winds. The surface to 700-hPa layer vertical shear is $\sim 5 \times 10^{-3}$ s^{-1}, with a bulk Richardson number of ~50. Notably absent from the sounding is the typical trade wind inversion, normally present between 2.0 and 2.5 km above sea level (Grindinger 1992). Although severe weather was not observed in the Hawaiian Islands on 3 November (UTC), heavy rainfall did occur over the island of Kauai, with 24-h rainfall totals as high as 263 mm (>10 in.).

By 0000 UTC 4 November 1995, the cold low at 250 hPa (Fig. 1b) is cut off from the main belt of the polar westerlies and enhanced upper-tropospheric divergence is present over the northwesternmost islands of Kauai and Oahu. The RSM 24-h forecast for 700 hPa valid at this time shows a jet of 27 m s^{-1} (55 kt) and cold/dry air advection to the west of the island of Kauai (Fig. 5a). These model features are not inconsistent with dynamic forcing associated with the jet entrance region aloft over this region (Fig. 1b) (Uccellini and Johnson 1979). The water vapor image for 0001 UTC on 4 November shows a woundup system with ribbons of moist and dry air encircling each other in the secluded core of the cold low aloft (Fig. 3b). On the southeast side of the kona low a finger of markedly drier air is penetrating northeastward just to the west of the anvil outflow associated with the bow-echo squall line. A minimum in θ_e at midlevels in the model atmosphere (Fig. 5b) is consistent with midlevel advection of cooler, drier air. Anticyclonic shear associated with the approaching kona low circulation contributes to the presence of conditional symmetric instability (Emanuel 1983; Hoskins et al. 1985) up to 300 mb across the northwest side of the cross section of the RSM model atmo-

[3] The RSM forecasts output at 10-km resolution and through 72 h became operationally available at the WSFO HNL in the summer of 1997.

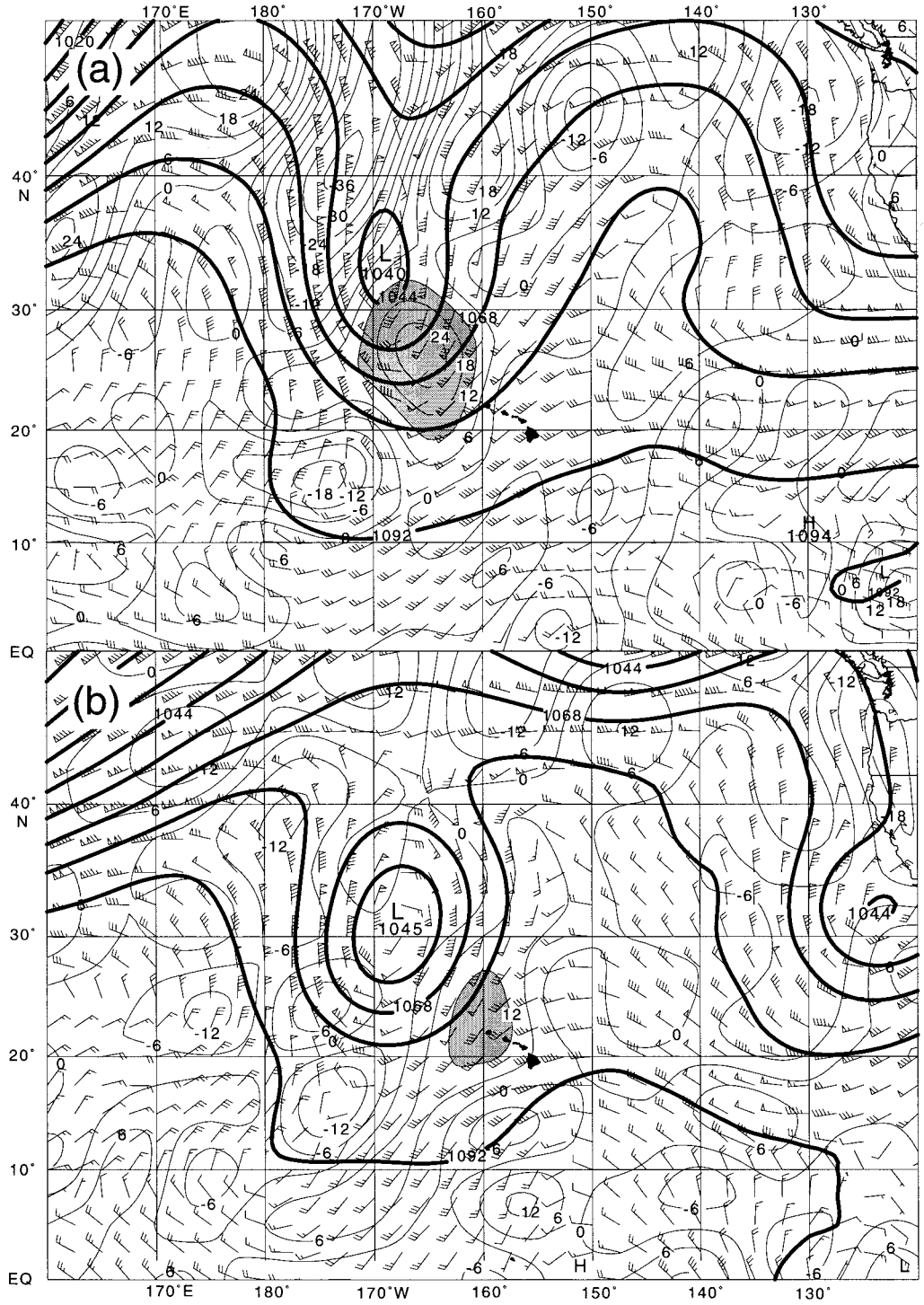

FIG. 1. The 250-hPa analyses based on aviation (AVN) model initialization for 0000 UTC on (a) 3 November 1995 and (b) 4 November 1995. Objectively analyzed heights (contour interval: 12 dam), wind velocity (full barbs are 5 m s^{-1}, half barbs are 2.5 m s^{-1}), and divergence (contour interval: 6×10^{-6} s^{-1}, values $> 12 \times 10^{-6}$ s^{-1}).

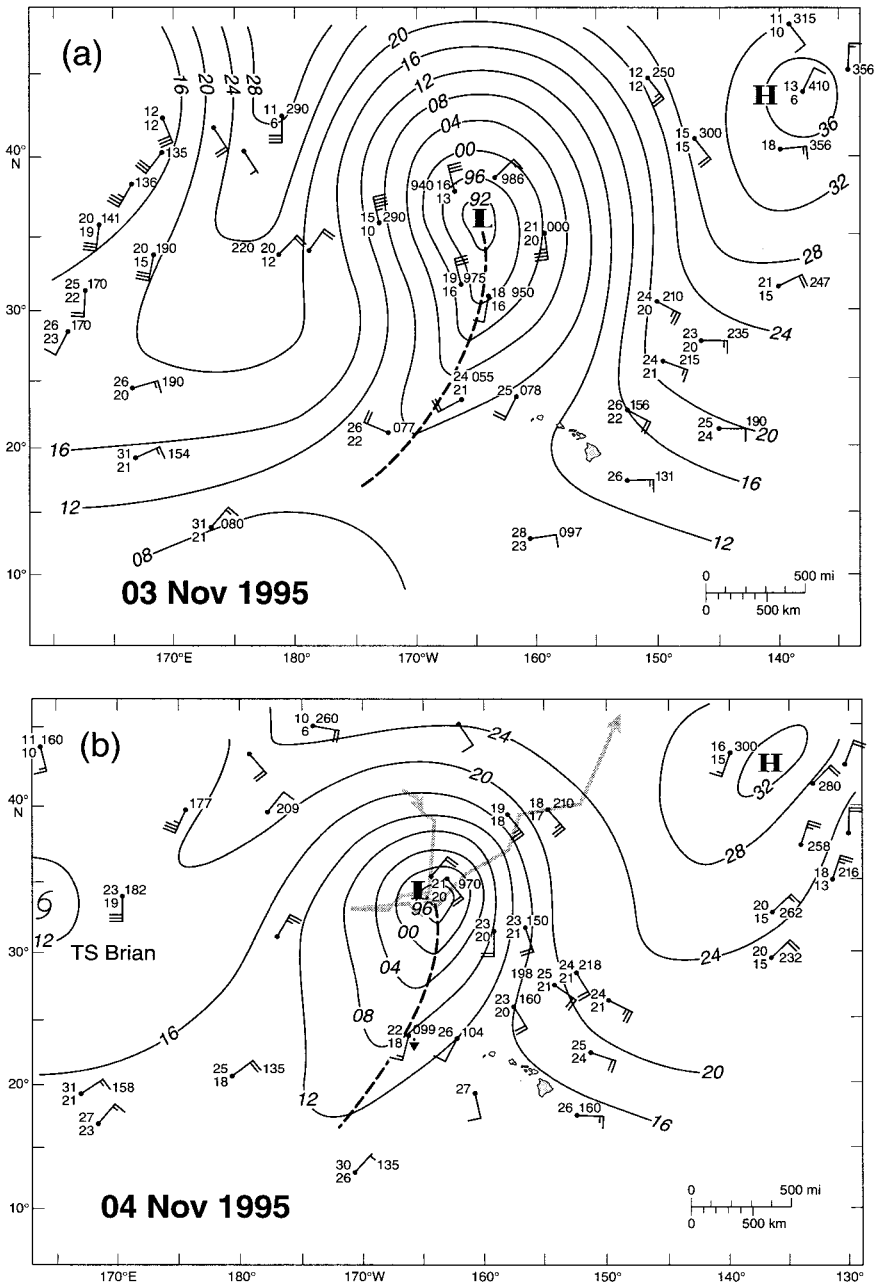

FIG. 2. Sea level pressure (hPa) analyses for 0000 UTC on (a) 3 November 1995 and (b) 4 November 1995. Ship observations are ±6 h from valid time and use standard plotting conventions. The 48-h track of the surface low starting at 1200 UTC 2 November is given by the heavy gray line in (b).

sphere (shading in Fig. 5b), consistent with convective bands present in the real and model atmospheres in this region (see Wang et al. 1998).

The corresponding surface analysis (Fig. 2b) shows the surface low center has tracked in a looping fashion to nearly the same position over the 24-h period, while the trailing anticyclone has shifted north of the surface cyclone, cutting off its source of cold polar air. Consequently, the cyclone has undergone slow filling (central pressure of 996 hPa), as expected of a fully occluded system undergoing frontolysis. The more uniform level of moisture seen in the core of the low aloft in the water vapor *GOES-9* imagery from 0001 UTC 4 November 1995 is indicative of a filling process (Fig. 3b). Nevertheless, this image and enhanced infrared imagery (not shown) for this time show convective bands to the north and west of the island chain, with cloud-top temperatures as low as −70° to −80°C.

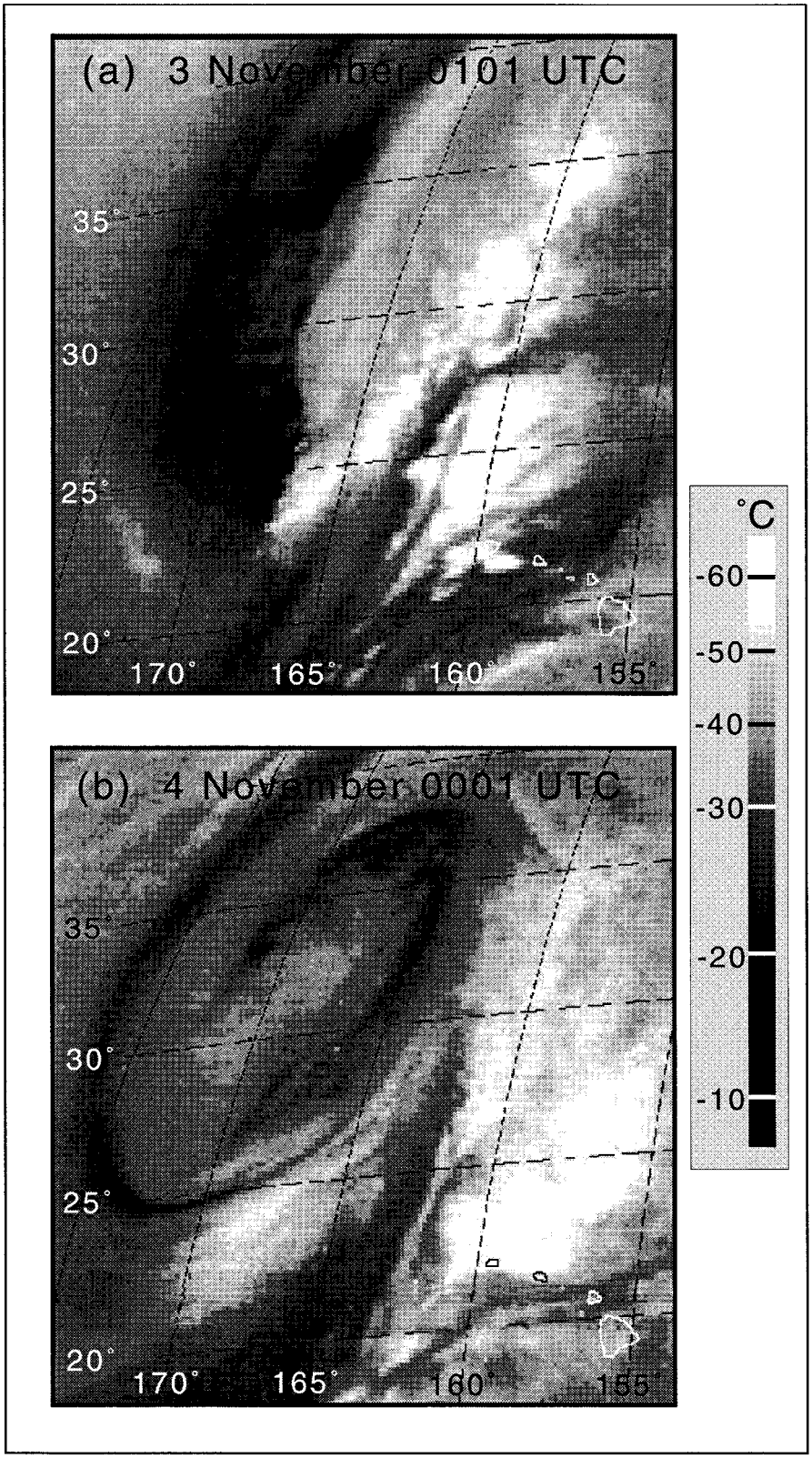

FIG. 3. *GOES-7* water vapor channel (6.7-μm wavelength) image for (a) 0101 UTC on 3 November 1995 and (b) 0001 UTC on 4 November 1995. Image resolution is 16 km.

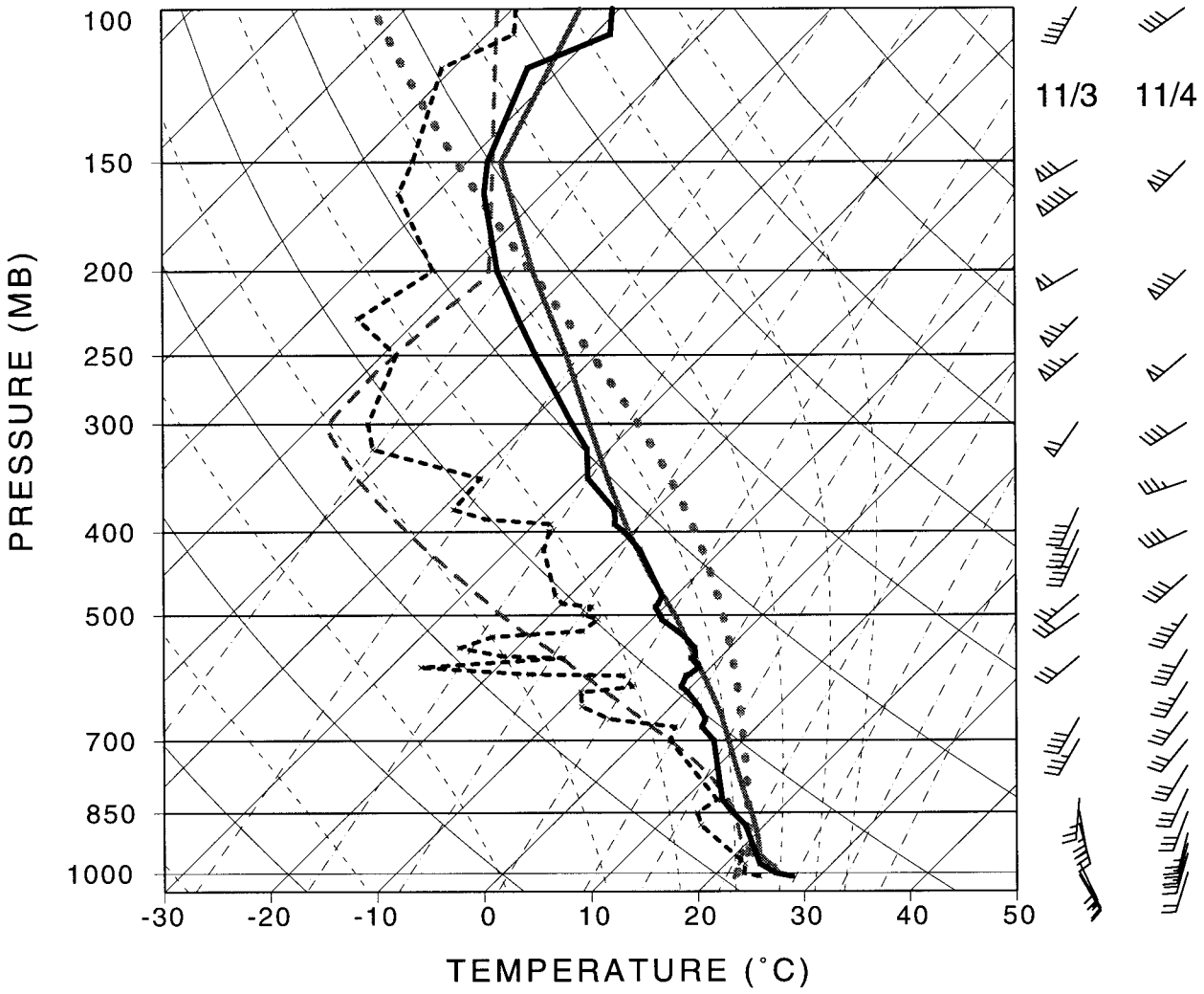

FIG. 4. Temperature (solid) and dewpoint temperature (dashed) profiles from Lihue, Kauai (LIH), at 0000 UTC 3 November 1995 (heavy black) and from RSM 24-h forecast valid 0000 UTC 4 November 1995 at 21°N, 161°W (dark gray). Dotted gray line shows the temperature profile of a rising surface-based parcel at 0000 UTC 4 November. Wind barbs as in Fig. 1.

As mentioned previously, soundings from Lihue, Kauai, for 1200 and 0000 UTC 4 November 1995 (~60 km east of the bow echo) are not available. Thus, a replacement sounding was constructed with output from the 24-h RSM forecast valid 0000 UTC 4 November to help reconstruct the prestorm environment (Fig. 4). The RSM thermodynamic profile shows drying in the mid-levels of the troposphere has occurred during the previous 24 h with little change in the temperature profile. The moist layer extends above 850 hPa, with surface-based air parcels reaching their level of free convection near 850 hPa and remaining buoyant to the tropopause, with a CAPE of 1412 J kg^{-1}. This value is of the same magnitude as reported by Jorgensen et al. (1997).

RSM model winds in the layer from the surface to 700 hPa layer indicate that the speed shear in this layer is only ~5 m s^{-1}, with a minimal amount of directional shear. Greater shear occurs in the region of a 700-mb wind maximum farther west (Fig. 5b). Winds of 30 m s^{-1} and surface to 700-mb shear of >20 m s^{-1} are found ~200 km northwest of the squall-line location (Fig. 5). It is our opinion, as supported by the radar velocity data presented in section 3, that significant wind shear did exist at the location of bow-echo formation. The fact that the enhanced shear in the RSM output is located too far to the west may be a result of a lack of wind data over the central Pacific in the initial state of the AVN, which provides the initial and boundary conditions to the RSM. The shortcomings of the RSM model wind forecast in this case underscores the importance of WSR-88D radar data to short-term forecasting in Hawaii in this case, and in similar cases in the future.

RSM output (Figs. 4 and 5b) suggests that the greatest drying is taking place in midtropospheric levels, a circumstance that has been previously linked to squall-line formation and severe weather outbreaks in extratropical

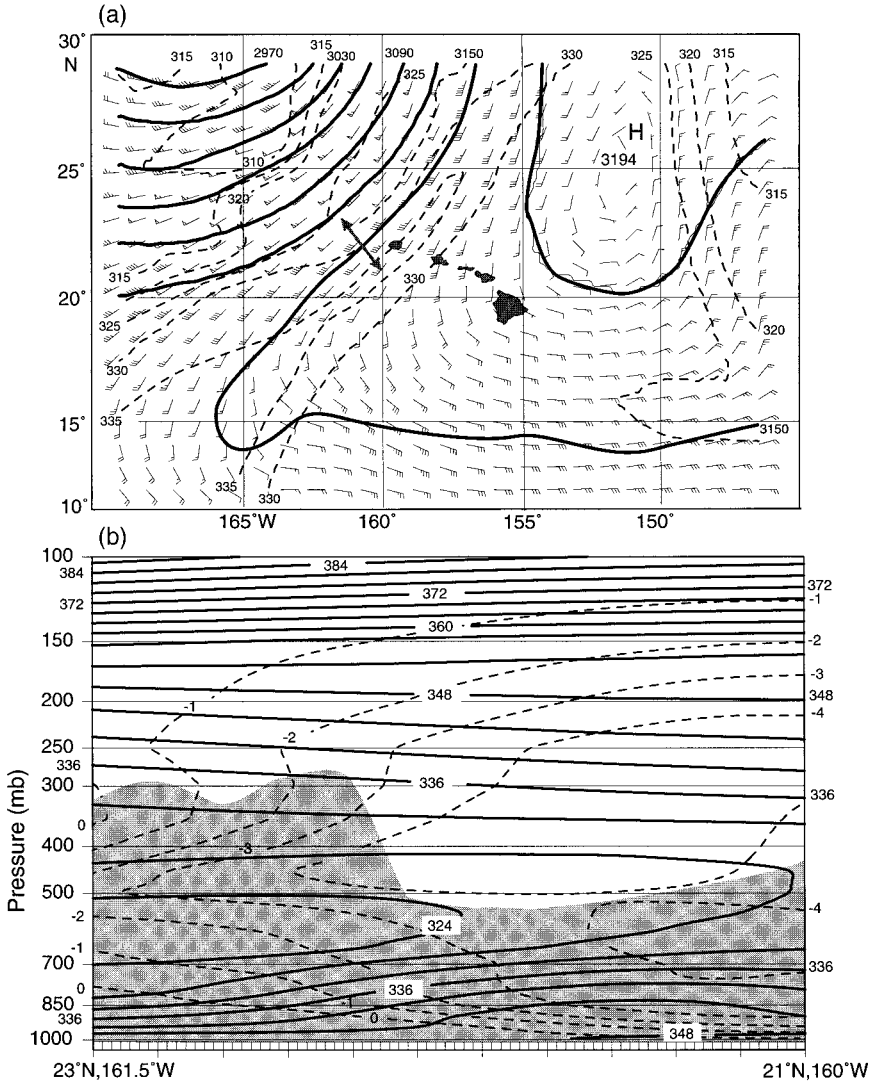

FIG. 5. RSM 24-h forecast valid 0000 UTC 4 November 1995 indicating (a) 700-hPa heights (contour interval 30 m), wind barbs (as in Fig. 1), and θ values (contour interval: 5 K). Location of the cross section in Fig. 5b is indicated by the gray arrow: (b) Vertical cross section of θ_e values (contour interval 4 K) and omega (contour interval: 1 μbar s^{-1}). Area of negative equivalent potential vorticity is shaded.

cyclones (Miller 1975; Hobbs et al. 1990; Businger et al. 1991; Locatelli et al. 1995). At 0037 UTC 4 November a squall line was observed by the Advanced Very High Resolution Radiometer (AVHRR) on the *NOAA-14* polar orbiting satellite. The visible image (0.63 μ) shows overshooting cloud tops associated with the squall line (arrow in Fig. 6). Clear, dry air is observed just to the northwest of the squall line (upper left of Fig. 6). The observed convective cloud distribution in Fig. 6 is consistent with the water vapor imagery in Fig. 3, which shows alternating bands of moist and dry air southwest of the low center, and with RSM output (Fig. 5), which indicates drier air advecting into the region at midtropospheric levels from the west.

3. Mesoscale analysis

The Kauai WSR-88D radar, located on the south side of the island at an elevation of 55 m (179 ft), observed bands of convection in the convergent southsouthwesterly airstream associated with the approaching kona low on the afternoon of 3 November Hawaiian standard time (HST). The radar imagery presented in this section is from the level III radar data archive[4] available to the forecaster at the time of the event. The squall line, seen in the AVHRR satellite imagery (Fig. 6), is observed

[4] Level II archive radar data are not available for this case.

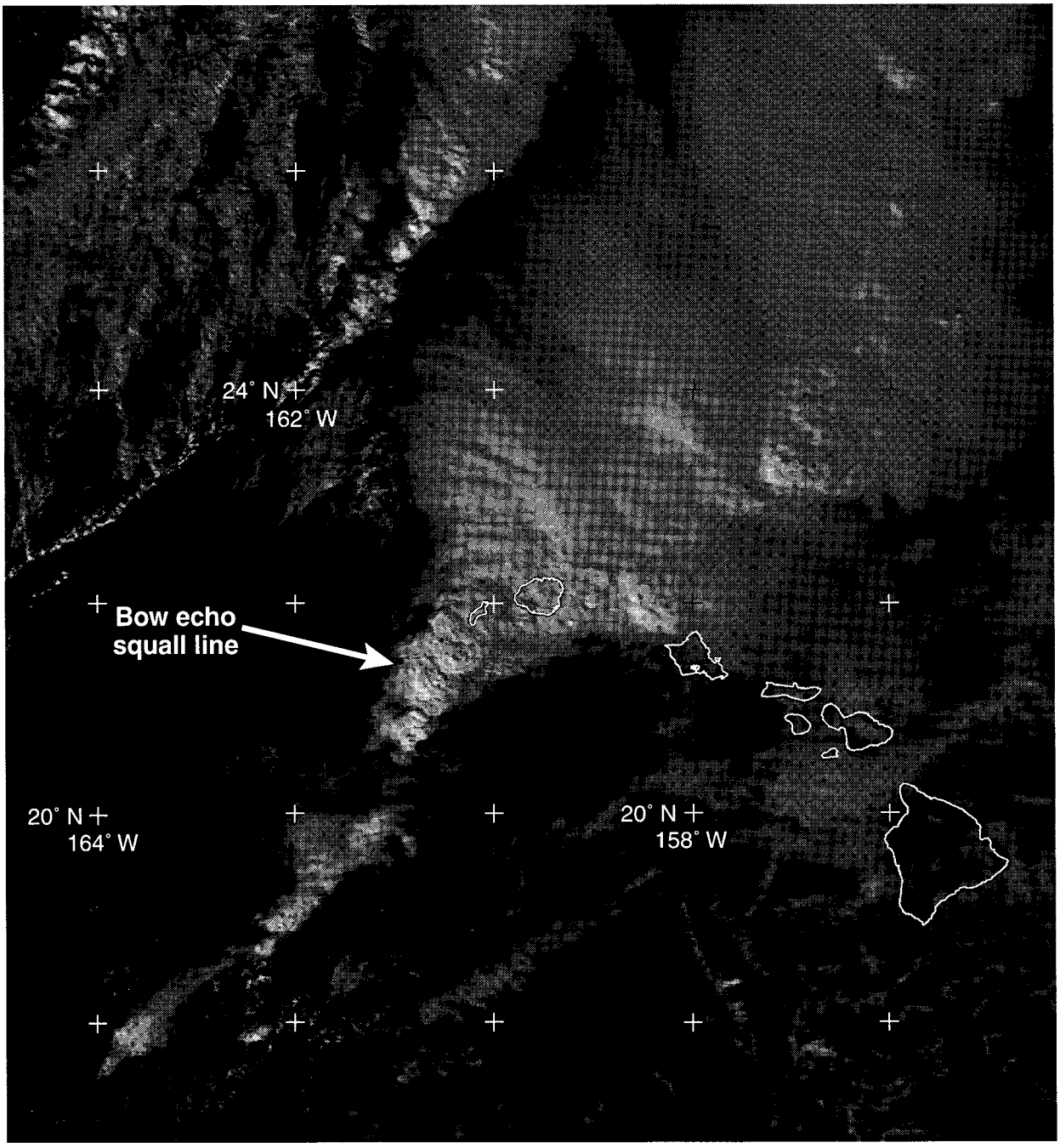

FIG. 6. AVHRR image of bow-echo squall line at 0037 UTC 4 November 1995 using visible wavelength (0.63 μm). Arrow indicates area of convection responsible for bow-echo development.

in the radar reflectivity imagery to propagate toward the eastnortheast at ~10 m s^{-1} with an orientation (NNE–SSW) nearly parallel to the low-level flow (Figs. 7 and 8). The squall line approached an area of weakening convection in the channel between Kauai and Niihau at 0000 UTC on 4 November (Fig. 7a) and interacted with residual outflow boundaries to form a north–south-oriented arc of enhanced convective precipitation (>50 dBZ in Fig. 7c). Evidence of enhanced rear inflow appears in the corresponding radial velocity images (Figs. 7b and 7d).

At 0136 UTC, a weak reflectivity notch appears in the rear flank of the arc (Fig. 7c). By 0240 UTC this storm displays classic bow-echo structure (Fujita 1978), with a sharp leading edge reflectivity gradient, a 26 m s^{-1} rear inflow jet, enhanced low-level convergence

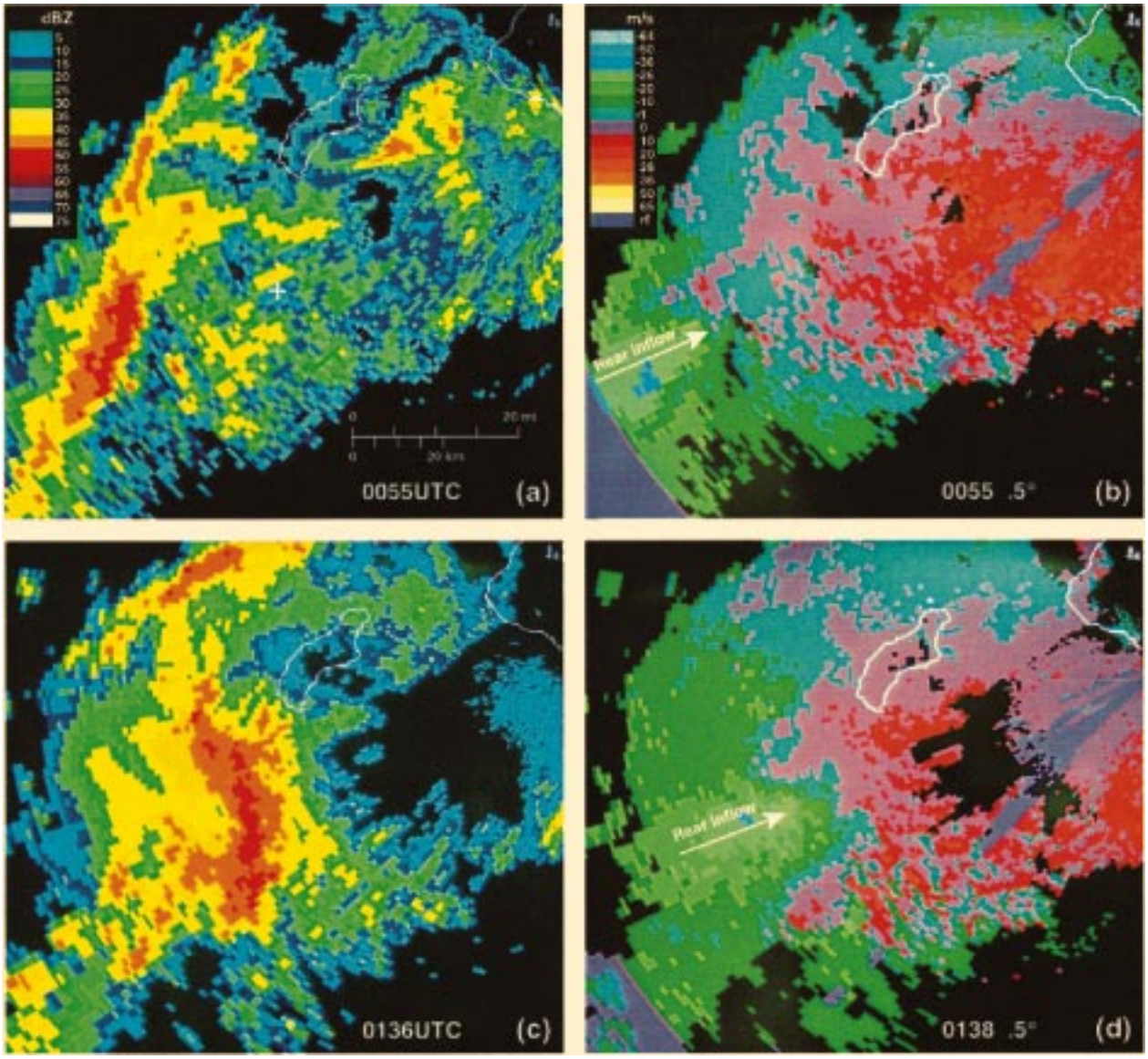

FIG. 7. WSR-88D equivalent base reflectivity (dBZ) for (a) 0055 and (c) 0136 UTC and radial velocity (m s^{-1}) for (b) 0055 and (d) 0136 UTC on 4 November 1995. Radar located on south Kauai, HI. Elevation angle is 0.5° with a resolution of 1 km (0.54 n mi). Arrows in (b) and (d) indicate regions of the rear inflow jet.

ahead of the line, and a bowing line segment (Figs. 8a and 8b). As drier, cooler air is advected into the rear of the system, a pronounced rear inflow notch appears (Smull and Houze 1987; Houze et al. 1989). In a review of bow-echo and derecho cases, Przybylinski (1995) showed that bow echoes and rear inflow notches are sometimes initially characterized by a hole of weak reflectivity, as observed in this case, which then evolves into a large rear inflow notch as the bowing segment develops. In the case presented here, two initially isolated rear inflow notches combine to form one larger rear inflow notch associated with the advancing bow echo (Figs. 8a and 8c).

Corresponding radial Doppler velocity images (Figs. 8b and 8d) indicate a mesocyclone signature in the cyclonic rotating *bookend* vortex, or comma head on the north end of the bow echo between Niihau and Kauai (Fujita 1978; Jorgensen and Smull 1993). This feature triggered a mesocyclone detection by the WSR-88D mesocyclone algorithm, indicating that the strength, depth, and duration of the mesocyclone circulation at this location warranted forecaster attention. Enhanced anticyclonic vorticity was also present on the southern flank of the inflow jet, suggesting a bookend vortex on the south end of the bow echo. However, the mesocyclone algorithm is not currently designed to detect mesoanticyclones.

A localized wind divergence characteristic of a down-

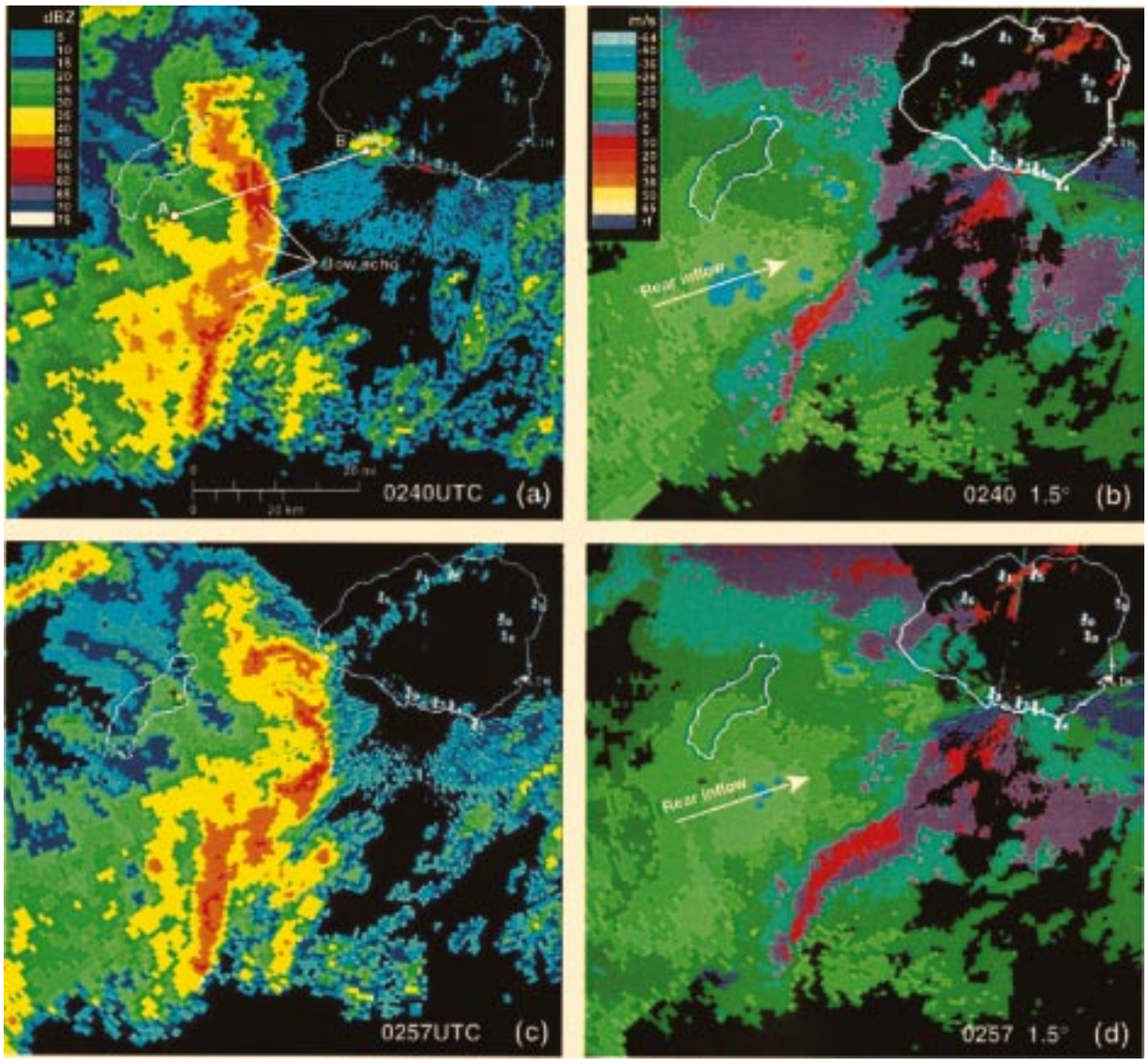

FIG. 8. WSR-88D equivalent base reflectivity (dBZ) for (a) 0240 and (c) 0257 UTC and radial velocity (m s^{-1}) for (b) 0240 and (d) 0257 UTC on 4 November 1995. Radar located on south Kauai, HI. Elevation angle is 1.5° with a resolution of 1 km (0.54 n mi). Line A–B in (a) indicates the location of the range–height cross section in Fig. 10. Arrows in (b) and (d) indicate regions of the rear inflow jet.

burst is seen in the radar radial wind field just south of the mesocyclone in the lowest (0.5°) elevation angle data at 0240 UTC (Fig. 9a). This feature appears again in the radar data for 0257 UTC, indicating a coherent event of some duration.

A reflectivity cross section taken through the bowing portion of the line at 0240 UTC (Fig. 10a) indicates thunderstorm tops reaching >13.5 km (45 000 ft). The strongest returns are located below the freezing level at a height of ~3.5 km (~12 000 ft), typical of tropical oceanic convective clouds that have been associated with relatively weak updrafts (Jorgensen and LeMone 1989), in contrast to those found in midlatitude continental convective cells (Houze et al. 1989; Zipser and Lutz 1994).

Figure 10b shows a cross section of the radial velocity relative to the radar taken through the bowing portion of the line at 0240 UTC and documents a 26 m s^{-1} (52 kt) jet descending from the rear of the system toward the location of the downburst, confirming the rear inflow jet as its source. Small radial velocities ahead of the line suggest the flow here is from the south-southeast, roughly at right angles to the radar beam. The leading edge of the bow echo was propagating at ~24 m s^{-1} toward the radar at this time. Low-level convergence in the plane of the cross section near the leading edge of the band is $\sim 4 \times 10^{-3}$ s^{-1}.

As the bow echo approached Kauai, the comma head portion broke away from the main bowing segment and

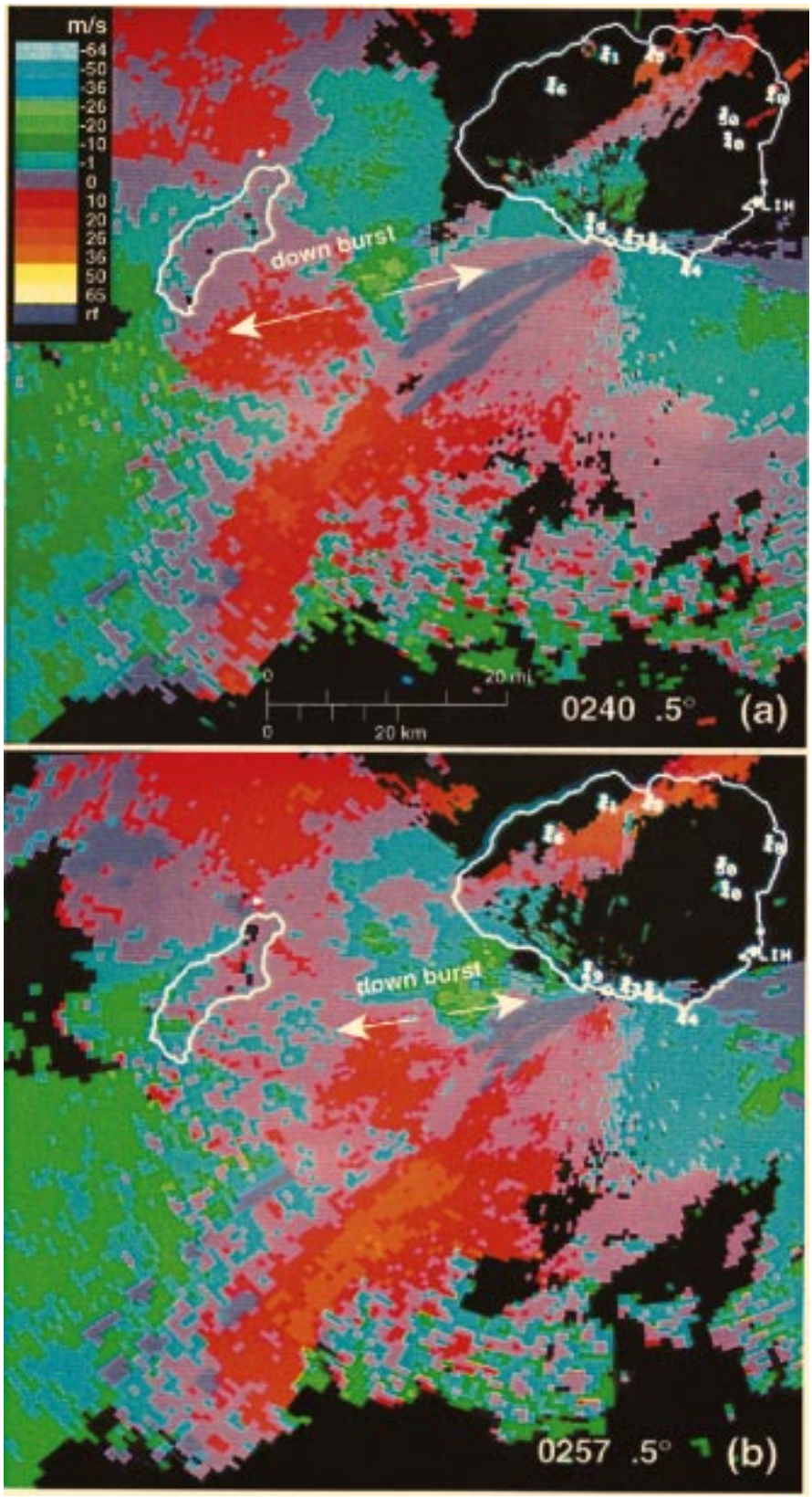

FIG. 9. WSR-88D radial velocity (m s^{-1}) for (a) 0240 and (b) 0257 UTC on 4 November 1995. Radar located on south Kauai, HI. Elevation angle is 0.5° with a resolution of 1 km (0.54 n mi). Arrows indicate regions of the downburst.

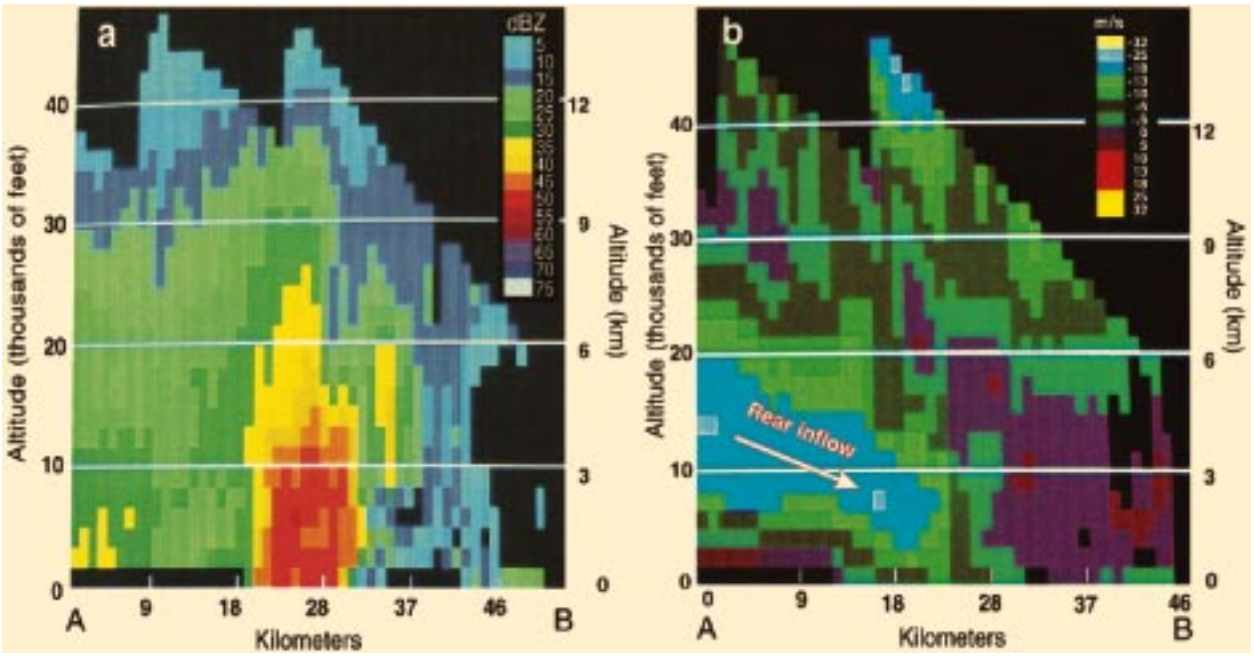

FIG. 10. WSR-88D range–height indicator cross section for 0240 UTC 4 November 1995, showing (a) equivalent base reflectivity (dBZ) and (b) radial velocity (m s^{-1}). The radial velocities depicted are toward and away from the radar and thus are not precisely parallel to the plane of the cross section.

moved northward along the steep cliffs of western Kauai (Polihale and the Na Pali coast) before dissipating. The bowing segment continued to propagate eastward along the south side of the island of Kauai toward the radar site. Damaging winds of 40 m s^{-1} (80 mph) were reported along the southeast shore of Kauai at approximately 0330 UTC. Although the bow echo appears to be weakening at this time, the system's evolution is difficult to interpret near the island because of terrain blockage of the lowest elevation angles of the radar. Terrain-related beam blockage affects approximately one-third of the surveillance area [from 310° to 80° azimuth; see Fig. 16 in Kodama and Businger (1998)].

4. Forecast considerations

The first notice of the possible threat of thunderstorms and heavy rainfall was given in a flood potential outlook (FPO) issued at 0700 UTC on 2 November 95 (2100 HST) (appendix B). This FPO was based on the presence of the strong subtropical cyclone to the northwest of the Hawaiian Islands, which forecasters recognized as a type of synoptic-scale system that is a notorious producer of thunderstorms, flash floods, and strong winds in the Hawaiian Islands. Forecasting the exact location and timing of flash flooding is difficult at best, but the potential for flooding on Kauai and Oahu was recognized by forecasters well in advance of the rain–wind event.

The primary model used for guidance in issuing the FPO was the aviation run of the GSM, which showed little movement of the low pressure system through the 72-h forecast. Subsequent runs of the GSM were consistent in the placement and movement of the low pressure center (nearly stationary), but deepened the central pressure with each successive run. Therefore, later forecasts maintained the threat of thunderstorm activity over Kauai and Oahu.

On the day of the bow-echo event, development of heavy showers and squall lines to the west and east of Kauai prompted the issuance of a flash flood watch for the entire island at 1800 UTC 3 November 1995. A flash flood warning was issued at 2000 UTC 3 November 1995, as convective lines moved onshore. These lines were observed by radar and satellite to merge over Kauai, resulting in heavy rains and flash flooding, primarily along the north and east sides of the island between 1900 UTC on 3 November 1995 and 0000 UTC on 4 November 1995.

Radar observations of the development of a bow echo approaching the south shore of Kauai from the west (Figs. 7–9), with the presence of a rear inflow jet of 26 m s^{-1} descending toward the surface, prompted the issuance of a severe thunderstorm warning, *a first for the NWS in Hawaii* (appendix A), and a special marine advisory valid from 0300 UTC to 0400 UTC on 4 November 1995. Later the warning was extended through 0430 UTC. At approximately 0330 UTC, the severe weather warning was verified, with reports of wind gusts to 40 m s^{-1} (80 kt). Convective-scale wind gusts tore the roof off the Nawiliwili Small Boat Harbor office (just south of Lihue) and knocked down trees and power

lines across portions of south and east Kauai. Given the mountainous character of Kauai, and the presence of an east–west-oriented ridge on the south side of the harbor, flow enhancement by the terrain cannot be discounted as a potential contributor to the high winds observed at Nawiliwili (e.g., Brinkmann 1974; Smith 1985; Mass et al. 1995).

The severe thunderstorm warning was issued with significant lead time and verified. This kind of warning performance would not have been possible without the WSR-88D observations. Although this is the first radar-documented case of severe weather in Hawaii, subsequent radar observations of the tropical Hawaiian atmosphere have confirmed that this was not an isolated event. In fact, several severe thunderstorm warnings have been issued for the Hawaiian Islands since the observation of the bow echo, with the WSR-88D indicating thunderstorm cells with supercell characteristics (see Kodama and Businger 1998; Pfost and Gerard 1997), and strong straight-line winds >25 m s^{-1}. Severe weather is not a recent development in Hawaiian weather; rather the WSR-88D allows meteorologists to observe mesoscale phenomena that occur on temporal and spatial scales that are too small to be observed by the previously available observing platforms. The significance of the impact of the WSR-88D radar observations on severe weather forecasting in Hawaii should not be underestimated. For example, the volume of air traffic in this tourist destination is considerable and particularly vulnerable to the impact of severe wind shears such as those documented in this case (e.g., Fujita and Byers 1977).

5. Summary and conclusions

During the first week of November 1995, a subtropical cyclone, or kona low, spawned a series of squall lines as it approached the Hawaiian islands from the northwest. As one of these convective bands approached the island of Kauai, it displayed pronounced bow-echo structure in reflectivity observations taken by a recently installed WSR-88D radar located on the south side of the island of Kauai. Recognition of the implications of the radar signatures led to the issuance of a severe thunderstorm warning, the first such warning ever issued by the National Weather Service Forecast Office in Honolulu, Hawaii (appendix A). Subsequent to the warning, winds of 40 m s^{-1} (80 kt) were observed at Nawiliwili Harbor on the southeast side of Kauai and convective-scale wind gusts tore the roof off the Nawiliwili Small Boat Harbor office and knocked down trees and power lines across portions of south and east Kauai.

The cold-core kona low developed as a product of the occlusion process of an extratropical wave cyclone that became secluded at lower latitudes by the blocking action of a warm high. A jet streak on the western side of the cold low aloft on 3 November contributed to the favorable dynamics at the time of squall-line formation on 4 November. Observational data and model output suggest that these conditions include enhanced divergence and cyclonic shear aloft (Fig. 1b), the likely presence of a wind maximum or jet (700 mb) resulting in enhanced midlevel advection of cool, dry air, and low-level wind shear, and a convergent southerly stream of moist, unstable air near the surface.

Output from the RSM 24-h forecast, currently available operationally with 10-km resolution in the WSFO-HNL, did not correctly predict the magnitude of environmental wind shear present at the location of the bow echo. The fact that the enhanced shear in the RSM output was located too far to the west may be a result of a lack of wind data over the central Pacific in the initial state of the AVN, which provides the initial and boundary conditions to the RSM. The shortcomings of the RSM model wind forecast in this case underscore the importance of WSR-88D radar data to short-term forecasting in Hawaii in this and in similar cases at this time.

By 0240 UTC on 4 November a classic bow-echo structure is seen in the radar reflectivity plan-position indicators (Fig. 8), with a sharp leading edge reflectivity gradient, a 26 m s^{-1} rear inflow jet with a pronounced rear inflow notch, enhanced low-level convergence ahead of the line, and a bowing line segment. Radar animation indicates counterrotating vortices on the northern and southern flanks of the bow echo, with a mesocyclone signature detected by radar algorithms on the north end of the bow echo.

The bow echo had a relatively short life span, compared to serial bow echoes modeled by Weisman (1992, 1993). Radar observations suggest the rear inflow jet descended rapidly to the ground and the convection-generated cold pool overwhelmed the ambient shear, resulting in short-lived, localized strong winds near the surface. It is hypothesized that less than optimal vertical shear and instability prevented the development of a longer-lived serial bow echo. The impact of the complex topography cannot be discounted in the storm's dissipation and the observed distribution of wind damage. These issues are the subject of further research.

The availability of WSR-88D data has increased the ability to sample the subtropical atmosphere and has provided forecasters and researchers with new insight into convective-scale phenomena near the Hawaiian Islands. Cases of mesoscale severe weather that were missed by the coarsely spaced synoptic network in the past have proven to be relatively common in radar observations of the otherwise data-sparse region surrounding the Hawaiian Islands.

Efforts are under way to use data derived from the WSR-88D radars, *GOES-9* satellite, and Global Positioning System receivers to enhance the initial state of a high-resolution nonhydrostatic version of the RSM in Hawaii (Wang et al. 1998). With the availability of data from geostationary and polar-orbiting satellites, GSM and RSM numerical output, and WSR-88D radar ob-

servations, the tools forecasters have to increase the accuracy of forecasts ranging from nowcasting to 48-h timescales are rapidly improving in the Pacific region.

Acknowledgments. The authors wish to extend their thanks to Dr. Gary Barnes for drawing attention to this unusual case and for his critical review of the manuscript. We also wish to thank John Porter for assistance with satellite data processing and James Partain for his motivation in shepherding the papers for the special issue. The authors are indebted to Arnold Hori, Tom Schroeder, Roger Pierce, Tom Heffner, Jim Weyman, and anonymous reviewers for their constructive contributions to this paper. This work has been supported by NOAA through the UCAR COMET Outreach Program under Grants UCAR S94-43844 and UCAR S97-86992 and the National Science Foundation through Grant ATM-9496335, SOEST Contribution number 4652.

APPENDIX A

Severe Thunderstorm Bulletin

WOHW42 PHNL 040300
HIZ002-040400-

BULLETIN - IMMEDIATE BROADCAST REQUESTED SEVERE THUNDERSTORM WARNING AND SPECIAL MARINE ADVISORY NATIONAL WEATHER SERVICE HONOLULU HI 500 PM HST FRI NOV 3 1995

. . . THE NATIONAL WEATHER SERVICE HAS ISSUED A SEVERE THUNDERSTORM WARNING EFFECTIVE UNTIL 6 PM FOR THE ISLAND OF KAUAI AND THE ADJACENT COASTAL WATERS . . .

AT 445 PM RADAR INDICATES A STRONG THUNDERSTORM JUST SOUTHWEST OF KAUAI MOVING NORTHEAST AT 25 MPH.

PERSONS ON KAUAI SHOULD BE READY FOR STRONG AND GUSTY WINDS FROM 50 TO 60 MPH WITH THIS THUNDERSTORM AS IT MOVES INTO KAUAI. VERY HEAVY RAINS AND DANGEROUS LIGHTNING WILL LIKELY ACCOMPANY THIS THUNDERSTORM. BOATERS ON WATERS ADJACENT TO KAUAI SHOULD BE PREPARED FOR STRONG AND ERRATIC WINDS WITH LOCALLY HIGH SEAS.

NATIONAL WEATHER SERVICE HONOLULU

APPENDIX B

Flood Potential Outlook

FLOOD POTENTIAL OUTLOOK
NATIONAL WEATHER SERVICE HONOLULU HI
9 PM HST WED NOV 01 1995

. . . HEAVY SHOWERS AND THUNDERSHOWERS ARE POSSIBLE OVER THE NEXT FEW DAYS ON ALL ISLANDS . . .

THE WEATHER PATTERN IS DEVELOPING INTO ONE THAT COULD PRODUCE HEAVY FLOOD PRODUCING RAINS OVER THE HAWAIIAN ISLANDS DURING THE NEXT FEW DAYS. THE ISLANDS MOST EXPOSED TO THIS THREAT OF HEAVY SHOWERS AND THUNDERSTORMS ARE KAUAI AND OAHU.

AN INTENSE LOW PRESSURE SYSTEM OF STORM INTENSITY HAS DEVELOPED TO THE NORTHWEST OF THE HAWAIIAN ISLANDS WHERE IT WILL REMAIN STATIONARY FOR A DAY OR TWO. THIS IS CAUSING MOIST TROPICAL AIR TO BE DRAWN NORTHWARD OVER THE CHAIN. THIS MOISTURE IS IN TURN BEING ACTED UPON BY THE DYNAMICS OF THE LOW PRESSURE SYSTEM WHICH WILL CAUSE A CLOUD BAND OF HEAVY SHOWERS TO FORM. THIS CLOUD BAND WILL AT FIRST AFFECT THE WESTERN ISLANDS OF KAUAI AND OAHU AND LATER ON THE OTHER ISLANDS ALSO. IN ADDITION LOCALIZED HEAVY SHOWERS WILL DEVELOP OUT AHEAD OF THE CLOUD BAND AND MOVE ACROSS THE ISLANDS FROM SOUTHERLY DIRECTIONS.

PRECISE TIMING OF THE WEATHER EVENTS AS THEY WILL OCCUR IS STILL UNCERTAIN. KEEP TABS ON THE WEATHER CONDITIONS OVER THE NEXT DAY OR TWO AND BE READY TO ACT QUICKLY IF FLOODING STARTS OR A WARNING IS ISSUED.

AN UPDATED OUTLOOK WILL BE ISSUED AT 9 AM THURSDAY OR SOONER IF NEEDED.

REFERENCES

Alfonso, A. P., and L. R. Naranjo, 1996: The 13 March 1993 severe squall line over western Cuba. *Wea. Forecasting,* **11,** 89–102.

Aspliden, C. I., Y. Tourre, and J. B. Sabine, 1976: Some climatological aspects of West African disturbance lines during GATE. *Mon. Wea. Rev.,* **104,** 1029–1035.

Barnes, G. M., and K. Sieckman, 1984: The environment of fast- and slow-moving tropical mesoscale convective cloud lines. *Mon. Wea. Rev.,* **112,** 1782–1794.

Brinkmann, W. A. R., 1974: Strong downslope winds at Boulder, Colorado. *Mon. Wea. Rev.,* **102,** 592–602.

Businger, S., B. H. Bauman III, and G. F. Watson, 1991: The development of the Piedmont front and associated outbreak of severe weather on 13 March 1986. *Mon. Wea. Rev.,* **119,** 2224–2251.

Chong, M., P. Amayenc, G. Scialom, and J. Testud, 1987: A tropical squall line observed during the COPT 81 experiment in West Africa. Part I: Kinematic structure inferred from dual-Doppler radar data. *Mon. Wea. Rev.,* **115,** 670–694.

Emanuel, K. A., 1983: On assessing local conditional symmetric instability from atmospheric soundings. *Mon. Wea. Rev.,* **111,** 2016–2033.

Fornander, A., 1996: *Ancient History of the Hawaiian People: To the times of Kamehameha I.* Mutual Publishing, 445 pp.

Fujita, T. T., 1978: Manual of downburst identification for Project NIMROD. Satellite and Mesometeorology Research Paper 156, Dept. of Geophysical Sciences, University of Chicago, 104 pp. [Available from Dept. of Geophys. Sci., University of Chicago, 5801 South Ellis, Chicago, Illinois 60637.]

——, and H. R. Byers, 1977: Spearhead echo and downburst in the crash of an airliner. *Mon. Wea. Rev.,* **105,** 129–146.

Grindinger, C. M., 1992: Temporal variability of the trade wind inversion: Measured with a boundary layer vertical profiler. M.S. thesis, Department of Meteorology, University of Hawaii, 93 pp. [Available from Department of Meteorology, Univ. of Hawaii, 2525 Correa Rd., HIG-331, Honolulu, HI 96822.]

Hobbs, P. V., J. D. Locatelli, and J. E. Martin, 1990: Cold fronts aloft and the forecasting of precipitation and severe weather east of the Rocky Mountains. *Wea. and Forecasting,* **5,** 613–626.

Hoskins, B. J., M. E. McIntyre, and A. W. Robertson, 1985: On the use and significance of isentropic potential vorticity maps. *Quart. J. Roy. Meteor. Soc.,* **111,** 877–946.

Houze, R. A., 1977: Structure and dynamics of a tropical squall-line system. *Mon. Wea. Rev.,* **105,** 1540–1567.

——, S. A. Rutledge, M. I. Biggerstaff, and B. F. Smull, 1989: Interpretation of Doppler weather radar displays of midlatitude mesoscale convective systems. *Bull. Amer. Meteor. Soc.,* **70,** 608–619.

Johns, R. H., 1993: Meteorological conditions associated with bow echo development in convective storms. *Wea. Forecasting,* **8,** 294–299.

——, and W. D. Hirt, 1987: Derechos: Widespread convectively induced windstorms. *Wea. Forecasting,* **2,** 32–49.

Jorgensen, D. P., and M. A. LeMone, 1989: Vertical velocity characteristics of oceanic convection. *J. Atmos. Sci.,* **46,** 621–640.

——, and B. F. Smull, 1993: Mesovortex circulations seen by airborne Doppler radar within a bow-echo MCS. *Bull. Amer. Meteor. Soc.,* **74,** 2146–2157.

——, M. A. LeMone, and S. B. Trier, 1997: Structure and evolution of the 22 February 1993 TOGA COARE squall line: Aircraft observations of precipitation, circulation, and surface energy fluxes. *J. Atmos. Sci.,* **54,** 1961–1985.

Juang, H.-M. H., and M. Kanamitsu, 1994: The NMC nested regional spectral model. *Mon. Wea. Rev.,* **122,** 3–26.

Keenan, T. D., and R. E. Carbone, 1992: A preliminary morphology of precipitation systems in northern Australia. *Quart. J. Roy. Meteor Soc.,* **118,** 283–326.

Knupp, K. R., 1996: Structure and evolution of a long-lived, microburst-producing storm. *Mon. Wea. Rev.,* **124,** 2785–2806.

Kodama, K. R., and G. M. Barnes, 1997: Heavy rain events over the south-facing slopes of Hawaii: Attendant conditions. *Wea. Forecasting,* **12,** 347–367.

——, and S. Businger, 1998: Weather and forecasting challenges in the Pacific Region of the National Weather Service. *Wea. Forecasting,* **13,** 253–276.

Lee, W. C., R. M. Wakimoto, and R. E. Carbone, 1992: The evolution and structure of a ''bow-echo microburst'' event. Part II: The bow echo. *Mon. Wea. Rev.,* **120,** 2211–2225.

Locatelli, J. D., J. E. Martin, J. A. Castle, and P. V. Hobbs, 1995: Structure and evolution of winter cyclones in the central United States and their effects on the distribution of precipitation. Part III: The development of a squall line associated with weak cold frontogenesis aloft. *Mon. Wea. Rev.,* **123,** 2641–2662.

Mass, C. F., S. Businger, M. D. Albright, and Z. A. Tucker, 1995: A windstorm in the lee of a gap in a coastal mountain barrier. *Mon. Wea. Rev.,* **123,** 315–331.

Miller, R. C., 1975: Notes on analysis and severe storm forecasting procedures of the Air Force Global Weather Central. Tech. Rep. 200 (revised), AWS, USAF. [Available from Headquarters AWS, Scott AFB, IL 62225.]

Nicholls, M. E., 1987: A comparison of the results of a two-dimensional numerical simulation of a tropical squall line with observations. *Mon. Wea. Rev.,* **115,** 3055–3077.

Nolen, R. H., 1959: A radar pattern associated with tornadoes. *Bull. Amer. Meteor. Soc.,* **40,** 277–279.

Pfost, R. L., and A. E. Gerard, 1997: ''Bookend vortex'' induced tornadoes along the Natchez Trace. *Wea. Forecasting,* **12,** 572–580.

Przybylinski, R. W., 1995: The bow echo: Observations, numerical simulations, and severe weather detection methods. *Wea. Forecasting,* **10,** 203–218.

Ramage, C. S., 1962: The subtropical cyclone. *J. Geophys. Res.,* **67,** 1401–1411.

——, 1995: Forecasters guide to tropical meteorology, AWS TR 240 Updated. AWS/TR-95/001, AWS, USAF, 392 pp. [Available from Headquarters AWS, Scott AFB, IL 62225.]

Roux, F., and S. Ju, 1990: Single-Doppler observations of a West African squall line on 27–28 May 1981 during COPT 81: Kinematics, thermodynamics and water budget. *Mon. Wea. Rev.,* **118,** 1826–1854.

Schroeder, T. A., 1977a: Meteorological analysis of an Oahu flood. *Mon. Wea. Rev.,* **105,** 458–468.

——, 1977b: Hawaiian waterspouts and tornadoes. *Mon. Wea. Rev.,* **105,** 1163–1170.

Simpson, R. H., 1952: Evolution of the Kona storm: A subtropical cyclone. *J. Meteor.,* **9,** 24–35.

Skamarock, W. C., M. L. Weisman, and J. B. Klemp, 1994: Three-dimensional evolution of simulated long-lived squall lines. *J. Atmos. Sci.,* **51,** 2563–2584.

Smith, R. B., 1985: On severe downslope winds. *J. Atmos. Sci.,* **42,** 2597–2603.

Smull, B. F., and R. A. Houze Jr., 1987: Rear inflow in squall lines with trailing stratiform precipitation. *Mon. Wea. Rev.,* **115,** 2869–2889.

Trier, S. B., W. C. Skamarock, M. A. Lemone, D. B. Parsons, and D. P. Jorgensen, 1996: Structure and evolution of the 22 February 1993 TOGA COARE squall line: Numerical simulations. *J. Atmos. Sci.,* **53,** 2861–2886.

——, ——, and ——, 1997: Structure and evolution of the 22 February 1993 TOGA COARE squall line: Organization mechanisms inferred from numerical simulation. *J. Atmos. Sci.,* **54,** 386–407.

Uccellini, L. W., and D. R. Johnson, 1979: The coupling of upper and lower tropospheric jet streaks and implications for the development of severe convective storms. *Mon. Wea. Rev.,* **107,** 682–703.

Wang, J. J., H.-M. H. Juang, K. Kodama, S. Businger, Y. L. Chen, and J. Partain, 1998: Application of the NCEP Regional Spectral Model to improve mesoscale weather forecasts in Hawaii. *Wea. Forecasting,* **13,** 290–305.

Weisman, M. L., 1992: The role of convectively generated rear-inflow jets in the evolution of long-lived mesoconvective systems. *J. Atmos. Sci.,* **49,** 1826–1847.

——, 1993: The genesis of severe, long-lived bow echoes. *J. Atmos. Sci.,* **50,** 645–670.

——, and J. B. Klemp, 1982: The dependence of numerically simulated convective storms on vertical wind shear and buoyancy. *Mon. Wea. Rev.,* **110,** 504–520.

Zipser, E. J., 1977: Mesoscale and convective-scale downdrafts as distinct components of squall-line structure. *Mon. Wea. Rev.,* **105,** 1568–1589.

——, and K. R. Lutz, 1994: The vertical profile of radar reflectivity of convective cells: A strong indicator of intensity and lightning probability? *Mon. Wea. Rev.,* **122,** 1751–1759.